Optics Letters

Fuseless side-pump combiner for efficient fluoride-based double-clad fiber pumping

Sébastien Magnan-Saucier,[1,2,*] Simon Duval,[1,3] Charles Matte-Breton,[1] Yiğit Ozan Aydin,[1] Vincent Fortin,[1] Sophie LaRochelle,[1] Martin Bernier,[1] and Réal Vallée[1]

[1]Centre d'optique, photonique et laser (COPL), Université Laval, Quebec, Québec QC G1V 0A6, Canada
[2]Solutions Novika, La Pocatière, Québec G0R 1Z0, Canada
[3]Femtum Inc., Québec, Québec G1P 4P5, Canada
*Corresponding author: Sebastien.Magnan-Saucier.1@ulaval.ca

Received 2 September 2020; revised 18 September 2020; accepted 19 September 2020; posted 21 September 2020 (Doc. ID 409174); published 13 October 2020

We report a novel technique for side-pumping fluoride-based double-clad fibers, allowing a record coupling efficiency of 93% and a maximum power handling near 100 W at 981 nm. Our simple technique is based on wrapping a silica taper around a fluoride fiber and, therefore, does not require any complex fusion between these two dissimilar fibers. Under passive cooling, pump combiners made of undoped and erbium-doped fluoride fibers were successfully operated during several hours at respective incident powers of 91 and 44 W. Heat management issues and active cooling strategies are also discussed. This innovative combiner is a keystone towards the development of compact and robust high-power mid-infrared fiber lasers and amplifiers.

https://doi.org/10.1364/OL.409174

Over the last few years, the development of lasers operating in the mid-infrared (MIR), especially within the 3–5 μm spectral region, has showed a growing interest for several applications. Remote sensing, material processing, biological tissues ablation, and many other applications can indeed benefit from high power coherent light sources in this spectral bandwidth often referred to as the molecular fingerprint region [1–3].

A broad range of fluoride glass fiber lasers operating from the continuous wave to the femtosecond regimes has been demonstrated to date and proved to be suitable candidates for several specific tasks [4,5]. These lasers are bringing to the MIR their whole set of features, including their high brightness, compactness, ease of operation, direct pumping, and efficient emission. However, MIR fiber lasers are still limited in performance and not yet widely available outside research labs, mainly due to the lack of some key fluoride fiber-based components. Specifically, an important step to ruggedize those lasers is the development of an all-fiber side-pump combiner. Such a component is crucial for several laser systems, including MOPA amplifiers and laser cavities in linear or ring configurations, as it simplifies the architecture and mitigates many heat-related issues arising from end face pumping [5–7]. Another important asset of side-pumping compared to end face pumping emerges from the possibility to distribute the pump absorption uniformly along the gain fiber since, in principle, there is no limitation on the number of side-pump combiners that can be added along a given fiber length, in both co- and counter-propagating configurations. Moreover, using a side-pump combiner within the laser cavity can reduce the heating of the front-end (pump-side) fiber Bragg grating, which is well-known to cause output wavelength drift and power instabilities [4,6]. The addition of such combiners in dual pumping architectures could also result in significant improvements [8]. Clearly, an adequate side-pump combiner for fluoride-based fibers would allow for better heat load management, would help to simplify and ruggedize the laser layout, and would open new opportunities for power scaling.

In silica-based fiber lasers, many side-pumping techniques for double-clad fibers (DCFs) are now well mastered, including embedded v-grooves side-pumping, embedded-mirror side-pumping and angle-polished fiber fusion side-pumping, to name a few [9–15]. These techniques provide coupling efficiencies up to 96% and pumping powers higher than 400 W. On the other hand, fabrication of fluoride-based side-pump combiners is bringing several challenges. The main difficulty arises from the fact that the pigtailed silica fiber used to deliver the output of the pump diode must be coupled to a fluoride-based fiber. Those two materials possess drastically different physical properties, namely glass transition temperature and thermal expansion coefficient [16], which complicate splicing or side coupling fusion between both fibers.

In 2018, Schäfer *et al.* reported the development of the first fluoride-based side-pumping combiner for high power fiber lasers at 2.8 μm [17]. Using active cooling to maintain a low temperature, they were able to obtain an 83% coupling efficiency and to pump up to 84.5 W in a doped combiner and 100 W in an undoped combiner [7]. However, their approach relied on angle-polished fluoride fibers, fluoride/fluoride angled splices, and silica/fluoride splices, which are all highly challenging steps due to the physical and thermal properties of fluoride

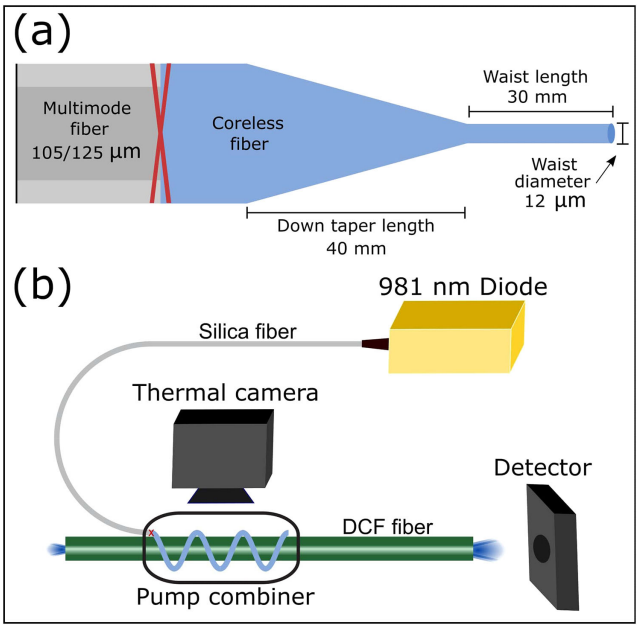

Fig. 1. (a) Taper profile. The red X denotes a splice between the 105/125 diode-pigtailed fiber and the coreless fiber used to make the 70 mm long taper. (b) Coupling efficiency setup used throughout the study to characterize the combiners.

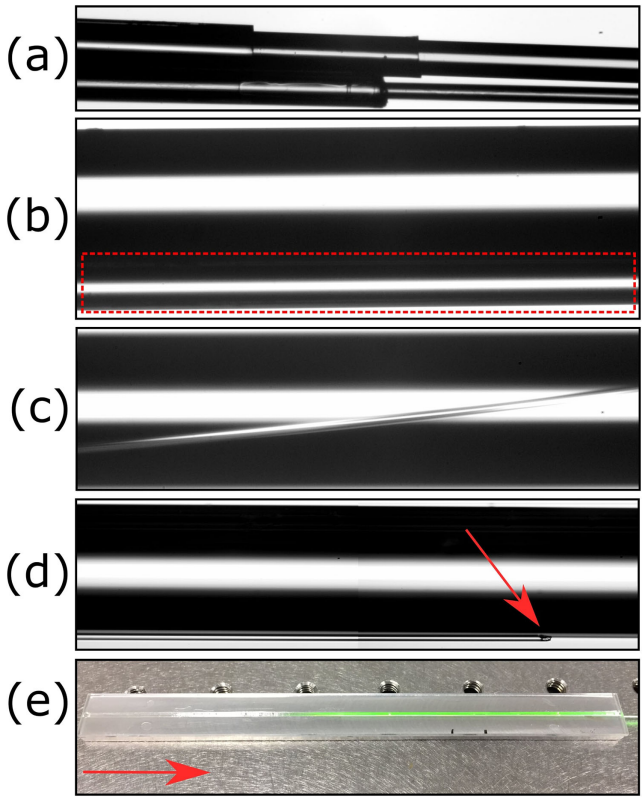

Fig. 2. Images showing the different sections of an erbium-doped combiner: (a) (microscope 5X) junction between the DCF and the silica fiber before the down-taper region; (b) (microscope 10X) the dotted box shows a portion of the down-taper region alongside the DCF; (c) (microscope 10X) waist region of the taper coiling along the DCF; (d) (microscope 25X) red arrow pointing at the end tip of the taper at the end of the waist region; and (e) packaged combiner made with an erbium-doped fluoride fiber while pumped at 981 nm. The red arrow indicates pumping direction.

glasses. Furthermore, the short coupling length of their angle-polished taper is believed to be a limitation for achieving higher efficiencies with this technique [18].

In this Letter, we introduce a simple fuseless fluoride-based side-pumping technique. Our side-pump combiners include silica tapers and do not need any fluoride glass fiber polishing or splicing. We obtained coupling efficiencies as high as 93% and maximum pump powers of 96 W while using passive cooling. These pump combiners could also be directly adapted to other types of fluoride or non-silica glasses, such as chalcogenides.

Two configurations of pump combiners were made by coupling tapered silica fibers to DCFs from *Le Verre Fluoré*. The first combiner is based on an undoped fluoride fiber with a diameter of 260 µm (NA > 0.46) and a core of 10 µm (NA = 0.19). The second combiner is made of a 7% erbium-doped D-shaped fluoride fiber (240 µm × 260 µm, NA > 0.46) and has a core of 15 µm (NA = 0.12). The fabrication technique was adapted from the one developed for the case of silica to silica fuseless side-pump combiners [19]. The first step consists of drawing a taper from a coreless 125 µm homemade silica fiber, using a CO_2 splicing device (Fujikura LZM-100). In order to distribute the heat load and to optimize the coupling efficiency, the precise design of the taper profile is critical. In this Letter, the coreless waist region is 30 mm long with a diameter of about 12 µm, the down taper is 40 mm long, whereas the up-taper portion (not shown) is of about 5 mm. Once the tapering is completed, the tapered fiber is cut so as to completely remove the up-taper portion, as shown in Fig. 1(a). The other end is then fusion spliced to the pigtail fiber (105/125 µm, NA = 0.22) of the 981 nm wavelength stabilized pump diode (BWT K9811AG1RN – 90 W).

The waist region is then placed alongside a DCF section that has previously been stripped from its polymer coating. A small amount of acetone is applied to improve the adhesion between both fibers by means of surface tension. In doing so, the tapered fiber naturally wraps around the DCF for approximately three turns. Once the acetone is evaporated (after a few seconds or so) the coupling efficiency is then monitored by launching a 981 nm signal through the silica fiber and by measuring the power at the output of the DCF using a thermopile detector (Gentec UP25N-250F-H12-D0) [Fig. 1(b)]. The temperature of the combiner is also monitored using a thermal camera (Jenoptik, Variocam). Figure 2 shows different microscope views of the assembly involving the silica taper and the fluoride DCF.

With slight adjustments of the position of both fibers, a coupling efficiency exceeding 85% is routinely achieved. In cases where the physical contact is limiting the coupling efficiency (e.g., the presence of polymer residues on the surface of the fiber or inadequate roll-up of the taper), one can simply remove the taper and redo the cleaning and coupling steps. The combiner can be immersed into a low-index polymer that is then cured on a metallic support to improve the coupling efficiency and to help maintaining the relative position between the fibers. [Fig. 2(e)].

The stability of the launched pump power over time was monitored for both undoped and doped combiners without any active cooling. The output of the undoped fluoride fiber

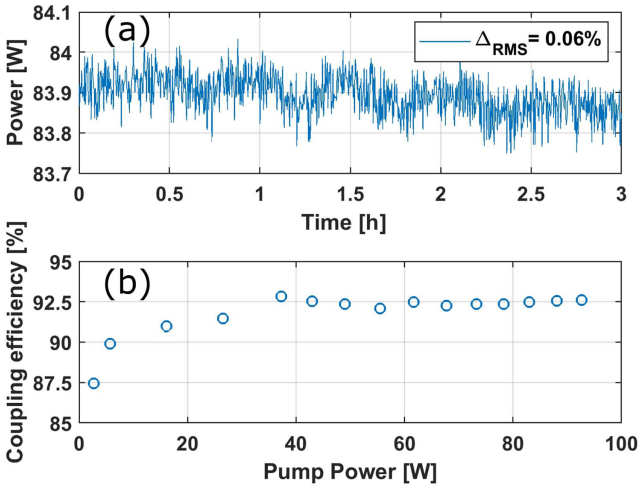

Fig. 3. (a) Output of the undoped fiber combiner over time while pumped with 90.8 W at 981 nm. Periodic fluctuations are caused by thermal variations in the laboratory due to air conditioning. (b) Coupling efficiency of the undoped combiner with respect to the pump power.

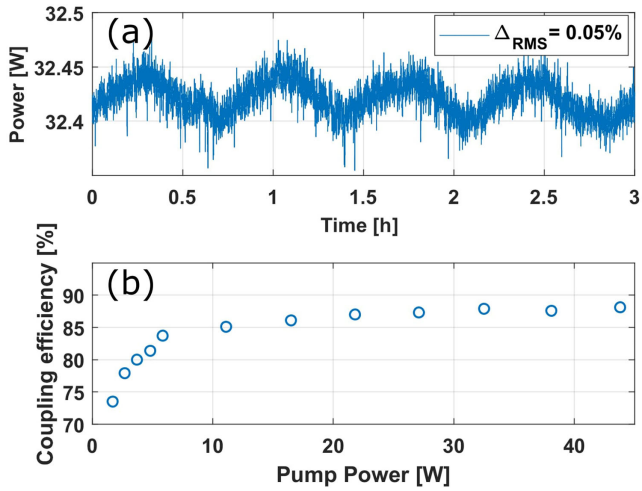

Fig. 4. (a) Output of the doped combiner over time while pumped with 44 W at 981 nm. Periodic fluctuation is caused by thermal variations in the laboratory due to air conditioning. (b) Coupling efficiency of the doped combiner with respect to the pump power once the erbium absorption is taken into account.

combiner was first measured during 3 h while pumping at 90.8 W and showed an RMS stability of 0.06% [see Fig. 3(a)]. A 48 h test (not shown) was also conducted at an incident pump power of 49 W and proved to be very stable (RMS = 0.05%). However, as one can see on Fig. 3, a subtle decrease of about 0.1% occurred during the 3 h acquisition. Such a behavior could be attributed to a change of the low-index polymer's properties due to excessive heating over a certain period of time. It is worth noting though that at maximum pumping power (96 W), the external temperature of the pump combiner packaging never exceeded 32°C. Figure 3(b) shows a slight increase of the coupling efficiency with the incident pump power, i.e., from 87.5% to 92.6%. The maximum efficiency is obtained by computing the ratio between the power detected at the output of the combiner and the power detected directly at the output of the pump diode pigtail, which was about 92.8%. This represents, to the best of our knowledge, the most efficient fluoride-based side-pumping combiner ever reported. For comparison, Schäfer *et al.* reported a maximum efficiency of 83%, but losses from their silica to fluoride splice were not considered [17].

The results for the erbium-doped fiber combiner are presented in Fig. 4. Note that the detected power is affected by the absorption of the erbium ions at 981 nm (i.e., about 2.5 dB/m). The actual efficiency of this combiner was evaluated after the experiment by performing a cutback procedure, and the maximum efficiency was found to be about 88.1% at 44 W pump power. To prevent lasing at 2.8 μm, both ends of this combiner were cleaved at a 10° angle. A stability measurement performed during a 3 h period showed RMS power fluctuations of 0.05% for an incident pump power of 44 W [see Fig. 4(a)]. Furthermore, the doped fiber combiner's efficiency was found to be more strongly dependent on the incident pumping power than in the undoped case [Fig. 4(b)]. This is most likely related to the heating of the erbium-doped fiber, which increases the temperature of the whole combiner packaging. During the experiment, the doped combiner's packaging reached 38°C while pumped at 62 W.

These results confirm that heat dissipation is one of the main concerns of such combiners. The fact that ZBLAN thermal expansion coefficient is about 30 times greater than that of silica is believed to have a noticeable impact on the coupling efficiency [16]. Despite this concern, the results are reproducible for each pump power, and corresponding efficiencies are recovered. We also observe that the coupling efficiency tends to a plateau as a function of pump power for both combiners. This situation might occur once the temperature is sufficiently high for the thermal expansion (of the fluoride glass) to completely bridge the gap between the silica taper and the fluoride fiber, incidentally reaching optimal coupling conditions. Additionally, in our case, the low-index polymer is most likely expanding with increasing temperature, which can affect the relative position between the tapered silica fiber and the fluoride fiber and thus modify the coupling efficiency.

To further assess the robustness of our combiners, rapid pump power variations (at 10 Hz with a 20% duty cycle and at 1 Hz with a 50% duty cycle) from 0 to 30 W were applied during more than one hour on a doped fiber combiner. The combiner output, as monitored with a silicon photodiode (Thorlabs FDS010, 1 ns rise time), is presented in Fig. 5 for both cases. Steady output average powers (ΔRMS < 0.2%) were measured (not shown) during a 60 min interval. Figure 5(c) shows a 50 ms wide pulse directly measured at the output of the pump diode (orange line) as well as at the output of the combiner (blue line), while the diode is pumping the combiner. One can infer from this plot that the combiner's response time is below the millisecond range.

Afterwards, to investigate the influence of the temperature on the combiner's efficiency, the aluminum groove temperature of the doped fiber combiner was actively controlled with Peltier modules (see Fig. 6). For a constant pump power of 30 W, the output power of the combiner was strongly correlated with temperature (erbium absorption is not considered in Fig. 6, since no cutback was performed for this doped combiner).

In this case, the output power varied from 15.4 to 13.2 W when the temperature was changed from 22.5°C to 30.2°C.

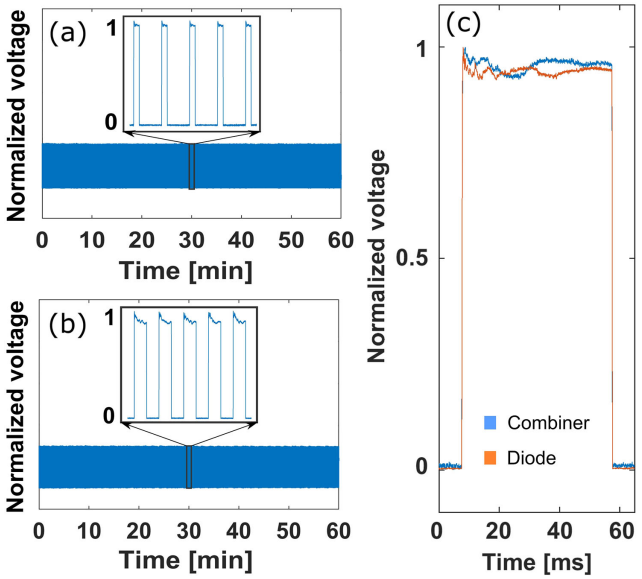

Fig. 5. Pump power cycles from 0 to 30 W applied to the doped fiber combiner. (a) More than 36,000 cycles were monitored at 10 Hz with a 20% duty cycle and; (b) more than 3600 cycles at 1 Hz with a 50% duty cycle. (c) Shape of a 50 ms pulse at the output of the pump diode (orange) and at the output of the combiner (blue).

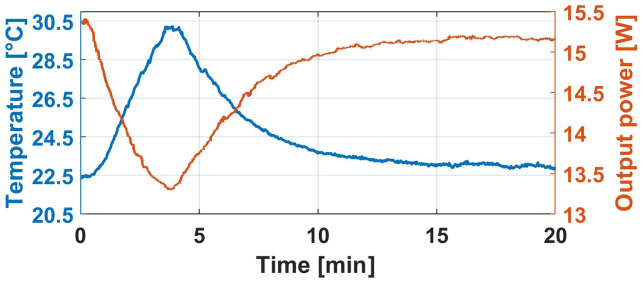

Fig. 6. Power at the output of a doped combiner with respect to the packaging temperature for a constant pumping power.

Since this 15% variation of the output power was achieved simply by controlling the packaging's temperature, one can conclude that active control of the temperature could henceforth be used to maintain an optimal coupling efficiency and ensure steady performances of the combiner over time while preventing any heat-related problems.

In this Letter, we proposed a novel and simple fuseless side-pump combiner for fluoride-based DCFs. Such a combiner does not require any polishing, fluoride to silica splices, nor fluoride to fluoride splices, which is a great asset for improved component robustness and reliability. While passively cooled, an efficiency as high as 93% and a power handling exceeding 96 W were obtained, approaching the best results achieved with all-silica side-pump combiners. The fuseless side-pump combiner presented here will facilitate the heat management in high power MIR fiber lasers, and will also simplify many lasers or amplifier architectures. In future works, active cooling technique and component design will be optimized in order to enhance and stabilize performances.

Funding. Canada First Research Excellence Fund (Sentinel North); Canada Foundation for Innovation (33240); Natural Sciences and Engineering Research Council of Canada (IRC-PJ469414); Fonds de recherche du Québec–Nature et technologies (2018-RS-203345, CO256655).

Acknowledgment. The authors would like to thank Marc D'Auteuil and Stephan Gagnon for technical assistance and Pascal Paradis for helpful discussions about signal processing.

Disclosures. SD: Femtum Inc. (I, E). SD, CMB, SL, MB, RV (P).

REFERENCES

1. F. K. Tittel, D. Richter, and A. Fried, in *Solid-State Mid-Infrared Laser Sources*, I. Sorokina and K. Vodopyanov, eds., Vol. **89** of Topics in Applied Physics (Springer, 2003), p. 458.
2. S. L. Johnson, M. R. Papantonakis, and R. F. Haglund, in *Laser-Surface Interactions for New Materials Production*, A. Miotello and P. M. Ossi, eds., Vol. **130** of Materials Science (Springer, 2010), p. 177.
3. S. Amini-Nik, D. Kraemer, M. L. Cowan, K. Gunaratne, P. Nadesan, B. A. Alman, and R. J. D. Miller, PLoS One **5**, e13053 (2010).
4. Y. O. Aydin, V. Fortin, R. Vallée, and M. Bernier, Opt. Lett. **43**, 4542 (2018).
5. S. Duval, M. Bernier, V. Fortin, J. Genest, M. Piché, and R. Vallée, Optica **2**, 623 (2015).
6. Y. O. Aydin, F. Maes, V. Fortin, S. T. Bah, R. Vallée, and M. Bernier, Opt. Express **27**, 20659 (2019).
7. H. Uehara, D. Konishi, K. Goya, R. Sahara, M. Murakami, and S. Tokita, Opt. Lett. **44**, 4777 (2019).
8. F. Maes, C. Stihler, L.-P. Pleau, V. Fortin, J. Limpert, M. Bernier, and R. Vallée, Opt. Express **27**, 2170 (2019).
9. D. J. Ripin and L. Goldberg, Electron. Lett. **31**, 2204 (1995).
10. J. P. Koplow, S. W. Moore, and D. A. V. Kliner, IEEE J. Quantum Electron. **39**, 529 (2003).
11. F. Hakimi and H. Hakimi, *Conference on Lasers and Electro-Optics* (2001), paper CTuD2.
12. Y. Sintov, Y. Glick, T. Koplowitch, O. Katz, Y. Nafcha, Y. Shamir, and R. Lavi, Proc. SPIE **6552**, 65520R (2007).
13. Q. Xiao, P. Yan, H. Ren, X. Chen, and M. Gong, J. Lightwave Technol. **31**, 2715 (2013).
14. T. Theeg, H. Sayinc, J. Neumann, L. Overmeyer, and D. Kracht, Opt. Express **20**, 28125 (2012).
15. C. Jauregui, S. Böhme, G. Wenetiadis, J. Limpert, and A. Tünnermann, J. Opt. Soc. Am. B **27**, 1011 (2010).
16. X. Zhu and N. Peyghambarian, Adv. OptoElectron. **2010**, 501956 (2010).
17. C. A. Schäfer, H. Uehara, D. Konishi, S. Hattori, H. Matsukuma, M. Murakami, S. Shimizu, and S. Tokita, Opt. Lett. **43**, 2340 (2018).
18. C. Lei, Z. Li, H. Zhang, Z. Chen, and J. Hou, Opt. Laser Technol. **130**, 106353 (2020).
19. C. Matte-Breton, R. Wang, Y. Messaddeq, and S. LaRochelle, *Optical Fiber Communication Conference (OFC)*, OSA Technical Digest (Optical Society of America, 2020), paper T3A.2.